GeoStudies

GeoStudies 3: 77–85 (2026)
DOI: 10.3897/geostudies.3.e207659

Research Article

Transient electromagnetic method (TEM) analysis and apparent resistivity interpretation: the importance of early-time sounding curve distortion

Michael Arvanitis[1]

1 *Geomorph Imaging Solutions Ltd, Nicosia, Cyprus*
Corresponding author: Michael Arvanitis (sales@geomorphimaging.com)

Abstract

Late-time apparent-resistivity expressions are widely used to transform transient electromagnetic (TEM) diffusion-field responses into resistivity sounding curves. At short delay times, however, the assumptions underlying the late-time approximation are not necessarily satisfied and the resulting apparent resistivities may be systematically distorted. This study quantifies that distortion for loop-source TEM configurations using analytical calculations and forward modelling over homogeneous and layered geoelectrical structures. The effects of transmitter-loop dimension, time delay, and subsurface resistivity are examined, and the transition from early- to late-time behaviour is expressed through a dimensionless diffusion-distance criterion. For the formulation tested, errors in late-time apparent resistivity fall below 5% when τ/a is approximately 13 or greater, and below 10% when τ/a exceeds approximately 10, where τ is the electromagnetic diffusion distance and a is the equivalent circular-loop radius related to the transmitter-loop side L through a = L/√π. Layered-model tests show that early-time deviations can reach approximately 44% and are most pronounced for larger loops and conductive near-surface conditions. Tabulated critical times and a worked example are provided for survey design, data quality control, and applications in which TEM apparent resistivity is used alongside plane-wave electromagnetic soundings or for magnetotelluric static-shift correction.

Key words: Transient electromagnetic method, apparent resistivity, early-time distortion, late-time approximation, loop-source TEM, magnetotelluric correction, sounding curve

OPEN ACCESS

Subject editor: Andrei Kosterov
Received: 13 July 2026
Accepted: 5 October 2026
Published: 20 October 2026

Citation: Arvanitis M (2026) Transient electromagnetic method (TEM) analysis and apparent resistivity interpretation: the importance of early-time sounding curve distortion. GeoStudies 3: 77–85. https://doi.org/10.3897/geostudies.3.e207659

Copyright: © Michael Arvanitis.
This is an open access article distributed under terms of the Creative Commons Attribution License (Attribution 4.0 International – CC BY 4.0).

Introduction

The transient electromagnetic (TEM) method is a time-domain electromagnetic technique widely used in mineral, hydrogeological, environmental, and engineering investigations because the time decay of the secondary field contains information on the subsurface electrical-resistivity distribution (Nabighian and Macnae 1991). Loop-source systems are particularly common in near-source TEM acquisition. Their response evolves from a source-geometry-dominated early-time regime toward a diffusion regime in which the transmitter can increasingly be approximated by a magnetic dipole.

Apparent resistivity provides an intuitive representation of TEM data, but its validity depends on the approximation used to convert the measured transient response. Early- and late-time transforms are not equivalent over the full decay, and an intermediate interval may exist in which neither asymptotic expression reproduces the true half-space resistivity accurately (Caldwell and Bibby 1998). Short-time distortion in coincident-loop measurements has also been demonstrated explicitly (Kamenetsky and Oelsner 2000). More generally, all-time imaging or direct inversion approaches have been developed partly because asymptotic apparent-resistivity transforms can become misleading outside their domains of validity (Christensen 2002).

Under simplified one-dimensional conditions, TEM and plane-wave electromagnetic soundings can display related resistivity trends. Transformations between MT frequency f and TEM delay time t have been used in joint interpretation, static-shift correction, and integrated near-surface geophysical surveys (Sternberg et al. 1988; Meju 1996, 1998; Arvanitis 2009):

$$194 / f = t \text{ (ms)} \tag{1}$$

$$1 / (3.9f) = t \text{ (s)} \tag{2}$$

TEM data used in such transformations are particularly sensitive to the choice of apparent-resistivity definition at early times. If a late-time expression is applied before the diffusion field has evolved sufficiently relative to the source dimension, the apparent-resistivity curve may acquire a systematic source-geometry-dependent bias. The objective of this study is therefore to quantify the onset of the late-time regime for loop-source TEM data, express the transition using a dimensionless criterion, and evaluate the implications for data selection and TEM–MT integration.

TEM geometry and sounding data analysis

In this study, a central-loop TEM configuration is employed, in which a square transmitter loop of side length L is laid out on the ground surface and a receiver coil (Rx) is placed at its centre (Fig. 1). Because the analytical expressions for the transient response of a circular loop over a half-space are considerably simpler than for a square geometry, the square loop is replaced by an equivalent circular loop of radius a chosen so that both loops enclose the same area. This equal-area equivalence gives $a = L / \sqrt{\pi}$. For example, a square transmitter loop with L = 100 m corresponds to an equivalent circular-loop radius $a \approx 56.4$ m. The equivalence is standard practice in TEM data processing and interpretation (Nabighian and Macnae 1991).

The influence of transmitter-loop size was first evaluated for homogeneous half-spaces. Four loop dimensions (L = 20, 50, 100, and 200 m; equivalent radii $a \approx 11.3$, 28.2, 56.4, and 112.8 m) were tested over a 100 Ω·m half-space. Delay times were selected to span the early- to late-time transition and were sampled on a sequence representative of the time range used by the Geonics EM-37 system. The measured quantity was transformed to apparent resistivity using the late-time expression, allowing the approximation error to be isolated as a function of time and source dimension (Fig. 2).

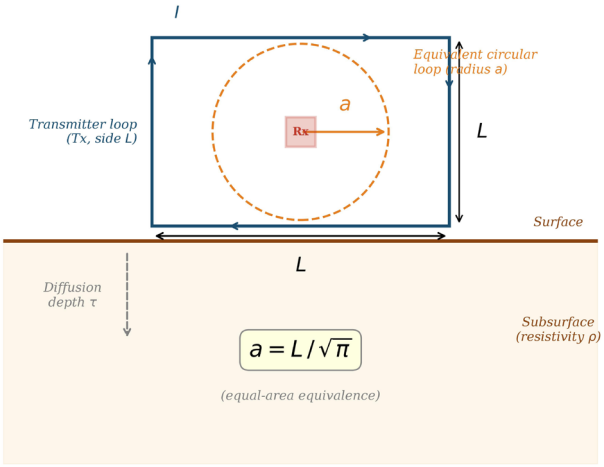

Figure 1. Central-loop TEM configuration. A square transmitter loop (Tx) of side length L carries current I. The dashed circle represents the equivalent circular loop of radius a = L/√π, having the same enclosed area. The receiver coil (Rx) is located at the centre of the array. Below the surface, the electromagnetic diffusion depth τ increases with time and subsurface resistivity ρ.

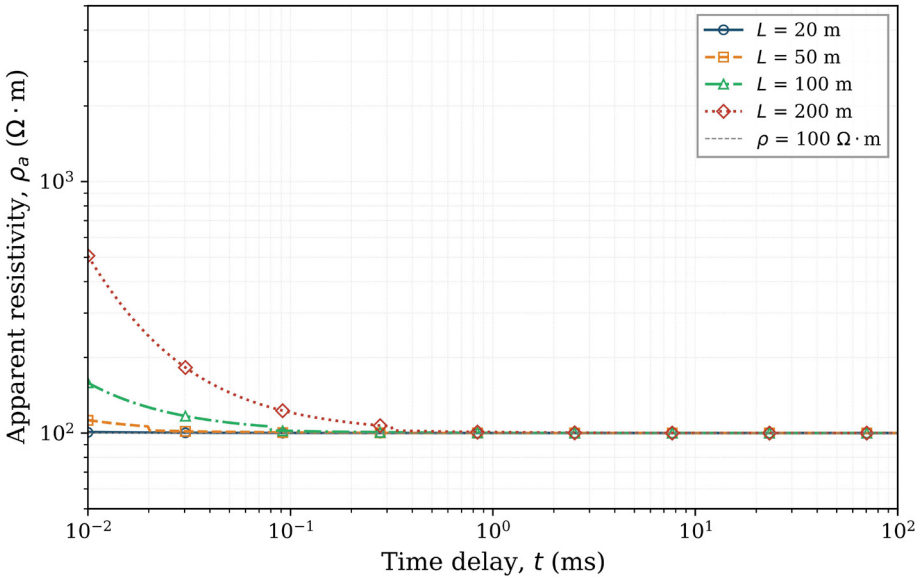

Figure 2. TEM apparent resistivity curves computed using the late-time formula for four different loop sizes (L = 20, 50, 100, and 200 m; equivalent radii a ≈ 11.3, 28.2, 56.4, and 112.8 m) over a homogeneous half-space with ρ = 100 Ω·m. Early-time distortion increases with loop size; all curves converge to the true resistivity at late times.

Figure 2 shows a strong loop-size dependence at short delay times. Larger loops produce greater apparent-resistivity overestimation when the late-time transform is applied early in the decay. With increasing delay time, the curves converge toward the true half-space resistivity. This behaviour is consistent with the progressive increase of electromagnetic diffusion distance relative to the transmitter dimension: only after the field has diffused sufficiently far from the source does the finite loop increasingly approach the dipole-source assumption underlying the late-time asymptote.

A second set of calculations was performed for a 50 Ω·m half-space using loop dimensions of 20, 50, 100, 200, and 500 m (Fig. 3). The same source-size dependence is observed, with the largest loop remaining outside the late-time regime for the longest interval. These results motivate a dimensionless description of the transition based on the ratio of electromagnetic diffusion distance to equivalent loop radius.

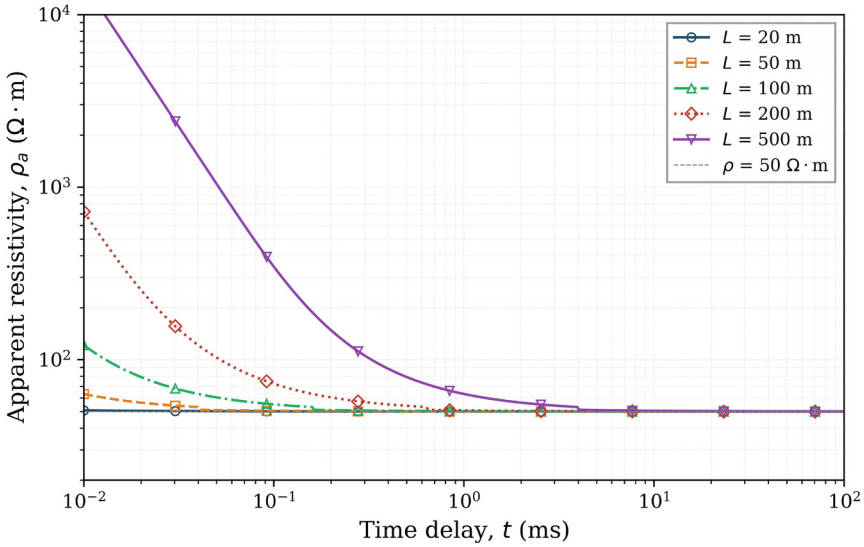

Figure 3. TEM apparent resistivity curves for five different loop sizes (L = 20, 50, 100, 200, and 500 m) over a homogeneous half-space with ρ = 50 Ω·m. The distortion magnitude scales with loop size and is most pronounced at early time delays.

Definition of the critical point

The time derivative of the magnetic field response (d*B*/d*t*) at the centre of a circular loop of radius *a* on a homogeneous half-space with resistivity ρ is expressed as:

$$\dot{B} = \frac{3I\rho}{a^3}\left[\Phi(u) - \sqrt{\frac{2}{\pi}}u\left(1+\frac{1}{3}u^2\right)e^{-u^2/2}\right] \tag{3}$$

In the late-time regime, the apparent resistivity is determined by:

$$\rho_\tau(\dot{B}) = \frac{\mu_0}{4\pi t}\left(\frac{2\pi I_0 a^2 \mu_0}{5t\dot{B}}\right)^{2/3} \tag{4}$$

where Φ(*u*) is the probability integral:

$$\Phi(u) = \sqrt{\frac{2}{\pi}}\int_0^{u(t)} e^{-t^2/2}\,dt \tag{5}$$

and the diffusion distance τ is defined as:

$$\tau = \sqrt{2\pi\rho t \times 10^7} \tag{6}$$

where ρ is the subsurface resistivity and *t* is the delay time. The parameter $u = 2\pi a/\tau$ relates the loop dimension to the diffusion distance.

Combining the above equations, the normalised apparent resistivity is given as:

$$\frac{\rho_\tau\left(\dot{B}\right)}{\rho} = 64.74\left[\Phi(u) - \sqrt{2/\pi}\,u\left(1+\frac{1}{3}u^2\right)e^{-u^2/2}\right]^{-2/3}\left(\frac{a}{\tau}\right)^{10/3} \tag{7}$$

In the late-time limit ($\tau/a \to \infty$, or equivalently $u \to 0$), the bracket term in Equation (3) tends to its leading Taylor expansion $\sqrt{(2/\pi)}\cdot u^5/15$, and Equation (7) reduces to $\rho\tau(\dot{B})/\rho = 1$, confirming that the late-time formula recovers the true half-space resistivity. At early times (small τ/a), the full response deviates from the late-time asymptote and the normalised ratio exceeds unity (Fig. 4).

The 5% error level was selected as the primary screening criterion because it is comparable to the typical repeatability and noise floor of modern TEM systems under favourable field conditions (Auken et al. 2003). The normalised apparent-resistivity response, evaluated as a function of τ/a, shows that the error of the late-time transform falls below 5% when τ/a exceeds approximately 13, and below 10% when τ/a exceeds approximately 10. Both thresholds are shown in Figure 4.

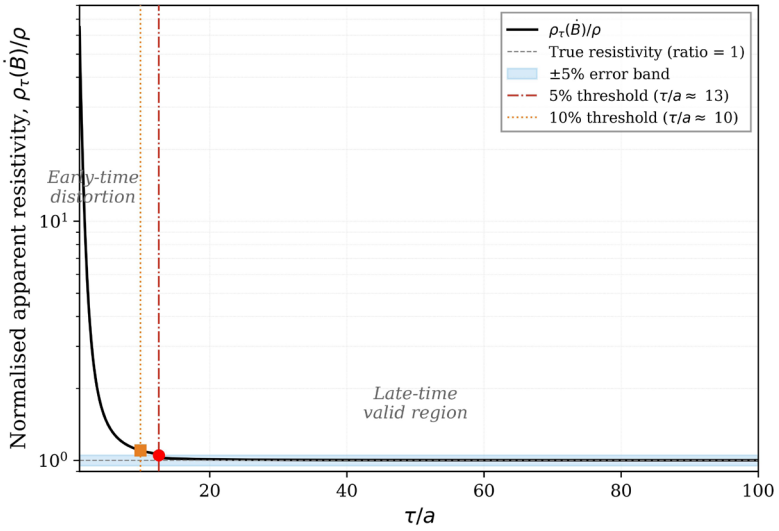

Figure 4. Normalised apparent resistivity ($\rho\tau(\dot{B})/\rho$) as a function of τ/a, computed from Equation (7). The curve decreases monotonically from large values at small τ/a (early-time distortion) toward unity at large τ/a (late-time convergence). The 5% error band (blue shading), the 5% threshold at $\tau/a \approx 13$ (red dot), and the 10% threshold at $\tau/a \approx 10$ (orange square) are indicated.

The critical late-time condition for the 5% threshold can be rewritten as:

$$\rho t \geq 13^2 \times a^2 / (2\pi \times 10^7) \tag{8}$$

or equivalently, expressing the critical time in milliseconds with a in kilometres:

$$t_{crit}\,(\text{ms}) \approx 2690\, a^2 / \rho \tag{9}$$

where a is the equivalent loop radius in km and ρ is in Ω·m. Because $a = L / \sqrt{\pi}$, any square-loop side length L can be directly converted. The corresponding critical times for various subsurface resistivities and loop sizes are listed in Table 1.

Table 1. Critical time tcrit (ms) for representative equivalent loop radii a (km) and corresponding square-loop side lengths L (m), computed from Equation (9) using the 5% error criterion (τ/a ≥ 13). Resistivities are in Ω·m. Data recorded at delay times shorter than tcrit are in the early-time regime and should be excluded from late-time interpretation or corrected using the full response formulation.

a (km)	L (m)	ρ=10	ρ=20	ρ=30	ρ=50	ρ=80	ρ=100	ρ=200	ρ=400	ρ=600
0.01	18	0.025	0.013	0.008	0.005	0.003	0.003	0.001	0.001	0.000
0.02	35	0.101	0.051	0.034	0.020	0.013	0.010	0.005	0.003	0.002
0.03	53	0.227	0.114	0.076	0.045	0.028	0.023	0.011	0.006	0.004
0.05	89	0.632	0.316	0.211	0.126	0.079	0.063	0.032	0.016	0.011
0.08	142	1.62	0.809	0.539	0.323	0.202	0.162	0.081	0.040	0.027
0.10	177	2.53	1.26	0.842	0.505	0.316	0.253	0.126	0.063	0.042
0.15	266	5.69	2.84	1.90	1.14	0.711	0.569	0.284	0.142	0.095
0.20	354	10.1	5.05	3.37	2.02	1.26	1.01	0.505	0.253	0.168

Practical example

To illustrate the use of Table 1, consider a field survey employing a square transmitter loop with L = 200 m over a site where the near-surface resistivity is estimated at ρ = 200 Ω·m. The equivalent circular-loop radius is $a = 200/\sqrt{\pi} \approx 112.8$ m = 0.113 km. From Equation (9), the critical time is:

$$t_{crit} = 2690 \times (0.113)^2 / 200 \approx 0.17 \text{ ms}$$

Figure 5 shows the TEM apparent-resistivity curve for this configuration. Data recorded at delay times shorter than $t_{crit} \approx 0.17$ ms lie in the early-time regime and are systematically distorted by the late-time formula. Only data at $t > t_{crit}$ should be used for late-time interpretation or for static-shift correction of magnetotelluric data. The 10% threshold occurs earlier, at approximately 0.10 ms, and may serve as a less conservative screening limit where higher noise levels make the additional precision unnecessary.

Distortion analysis and correction

The homogeneous-half-space analysis isolates the source-geometry effect, whereas practical TEM soundings frequently sample layered resistivity structures. To test the persistence of the distortion under vertical resistivity variation, descending-resistivity and ascending-resistivity layered models were evaluated over a range of near-surface resistivities. Full transient responses were compared with apparent-resistivity curves calculated using the late-time approximation.

The layered-model results show that early-time deviations can reach approximately 44% relative to the plane-wave reference response. The distortion diminishes as the response moves into the late-time regime, but the transition time depends on both loop size and resistivity structure. For the layered models, the time beyond which the discrepancy fell below 10% was also tracked as a secondary practical indicator. Correction was performed by recalculating the response from the full electromagnetic formulation rather than forcing the late-time asymptote across the complete decay.

The largest relative deviations occur for conductive near-surface conditions in the approximate 10–50 Ω·m range tested. In more resistive media the char-

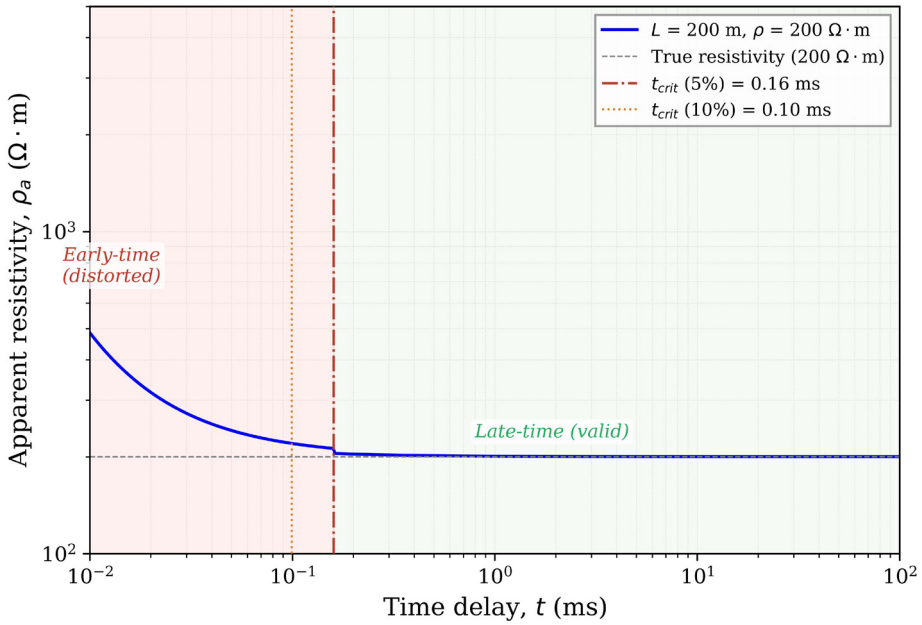

Figure 5. Practical application of the critical-time screening for a square transmitter loop with L = 200 m (a ≈ 112.8 m) over a 200 Ω·m half-space. The shaded regions indicate the early-time (distorted, red) and late-time (valid, green) intervals, separated by the critical times for the 5% criterion (tcrit ≈ 0.16 ms) and the 10% criterion (≈ 0.10 ms).

acteristic diffusion distance increases more rapidly with time, so the ratio τ/a reaches the late-time threshold earlier. Conductive near-surface layers prolong the interval over which the source geometry remains important. This trend is physically consistent with the source- and resistivity-dependence of near-source TEM responses reported in comparative modelling studies (Zhou et al. 2017).

Discussion

The results have several practical implications. First, apparent resistivity should not be treated as a source-independent observable at all delay times. The finite transmitter geometry can dominate the early response, and increasing loop dimension extends the time interval over which a late-time transform is biased. Large loops may still be desirable for signal amplitude and investigation depth, but those benefits do not remove the need to identify the valid time range of the selected transform.

Second, the τ/*a* criterion provides a dimensionless quality-control parameter for the idealised loop-source case. Rather than selecting a fixed early or late time in milliseconds, the criterion scales the delay time by source dimension and representative resistivity through diffusion distance. Data below the operational threshold should be interpreted with the full response, an appropriate all-time transform, or direct inversion. This is especially relevant when TEM curves are used to constrain MT static shifts, because a systematic early-time bias can be propagated into the corrected plane-wave resistivity curve (Sternberg et al. 1988; Meju 1996).

Third, Table 1 and the worked example in “Practical example” demonstrate how the screening criterion can be applied before or during data processing. The table is not a substitute for system-specific forward modelling: transmitter waveform, turn-off ramp, receiver transfer function, filtering, noise floor, and lat-

eral heterogeneity can modify the observed early-time response. Comparative near-source studies likewise emphasise that source configuration and full-response modelling are central to reliable interpretation (Zhou et al. 2017). The practical contribution of the present criterion is therefore as a transparent screening and quality-control tool, not as a replacement for inversion.

Fourth, the choice of 5% as the primary error threshold was motivated by the typical repeatability of field TEM data. Auken et al. (2003) reported data-quality assessments for modern TEM systems showing that uniform-half-space standard deviations of 3–5% are achievable under favourable noise conditions. A late-time distortion at the same level as the measurement noise is thus operationally negligible, whereas systematic biases exceeding this level can mislead the interpreter. Where field noise is higher, the 10% threshold ($\tau/a \approx 10$) may serve as a sufficient screening criterion.

Conclusions

This study examined the error introduced when a late-time apparent-resistivity approximation is applied to loop-source TEM data before the diffusion field has evolved sufficiently relative to the transmitter dimension. Homogeneous and layered models were used to isolate the effects of loop size, delay time, and electrical resistivity. The principal findings are as follows:

(1) Early-time TEM apparent resistivity curves exhibit systematic distortion when computed using late-time approximation formulae. The magnitude of this distortion increases with transmitter loop size and decreases with increasing subsurface resistivity.
(2) The transition from early-time to late-time regimes is described by the dimensionless ratio τ/a, where τ is the electromagnetic diffusion distance and $a = L/\sqrt{\pi}$ is the equivalent circular-loop radius for a square transmitter loop of side L. The late-time apparent resistivity enters the 5% error band at $\tau/a \approx 13$, and the 10% band at $\tau/a \approx 10$.
(3) Tabulated critical times for representative resistivities and loop sizes, together with a worked example, provide a practical reference for survey design and data quality assessment.
(4) The identified distortion has direct implications for the use of TEM data in correcting MT static shifts. Applying uncorrected early-time TEM apparent resistivities to MT data will propagate systematic errors into the final interpretation.

The proposed threshold is deliberately simple and can be calculated before or during processing. Future work should test the criterion against additional waveforms, receiver components, non-coincident geometries, multidimensional conductivity structures, and field datasets with accurately characterised system responses.

Acknowledgments

The author gratefully acknowledges the support of Geomorph Imaging Solutions Ltd during the preparation of this manuscript.

Additional information

Conflict of interest

The author has declared that no competing interests exist.

Ethical statement

No ethical statement was reported.

Artificial Intelligence (AI) use

The author accepts full responsibility for the content of the manuscript, including the disclosure of any use of AI.
No AI tools were used in the preparation of this manuscript.

Author ORCIDs

Michael Arvanitis https://orcid.org/0009-0003-6085-7276

Data availability

All of the data that support the findings of this study are available in the main text

References

Arvanitis M (2009) Modified Finslerian spaces for more effective ray-tracing. Application to seismic travel-time tomography. Central European Journal of Geosciences 1(4): 424–430. https://doi.org/10.2478/v10085-009-0033-4

Auken E, Jørgensen F, Sørensen KI (2003) Large-scale TEM investigation for groundwater. Exploration Geophysics 34(3): 188–194. https://doi.org/10.1071/EG03188

Caldwell TG, Bibby HM (1998) The instantaneous apparent resistivity tensor: a visualization scheme for LOTEM electric field measurements. Geophysical Journal International 135(3): 817–834. https://doi.org/10.1046/j.1365-246X.1998.00668.x

Christensen NB (2002) A generic 1-D imaging method for transient electromagnetic data. Geophysics 67(2): 438–447. https://doi.org/10.1190/1.1468603

Kamenetsky F, Oelsner ChR (2000) Distortions of EM transients in coincident loops at short time-delays. Geophysical Prospecting 48(6): 983–993. https://doi.org/10.1046/j.1365-2478.2000.00228.x

Meju MA (1996) Joint inversion of TEM and distorted MT soundings: Some effective practical considerations. Geophysics 61(1): 56–65. https://doi.org/10.1190/1.1443956

Meju MA (1998) A simple method of transient electromagnetic data analysis. Geophysics 63(2): 405–410. https://doi.org/10.1190/1.1444340

Nabighian MN, Macnae JC (1991) Time Domain Electromagnetic Prospecting Methods. In: Nabighian MN, Corbett JD (Eds) Electromagnetic Methods in Applied Geophysics, Volume 2, Chapter 6. https://doi.org/10.1190/1.9781560802686.ch6

Sternberg BK, Washburne JC, Pellerin L (1988) Correction for the static shift in magnetotellurics using transient electromagnetic soundings. Geophysics 53(11): 1459–1468. https://doi.org/10.1190/1.1442426

Zhou N, Xue G, Chen W, Cui J, Chen K (2017) A comparison of TEM data from different near-source systems. Journal of Geophysics and Engineering 14(3): 487–501. https://doi.org/10.1088/1742-2140/aa5cde.